Journal of Power Sources 247 (2014) 703–711

Contents lists available at ScienceDirect

Journal of Power Sources

journal homepage: www.elsevier.com/locate/jpowsour

Copper sulfides for rechargeable lithium batteries: Linking cycling stability to electrolyte composition

Birte Jache, Boris Mogwitz, Franziska Klein, Philipp Adelhelm*

Institute of Physical Chemistry, Justus-Liebig-University Giessen, Heinrich-Buff-Ring 58, 35392 Giessen, Germany

HIGHLIGHTS

- The reversibility of copper sulfides strongly depends on the electrolyte composition.
- Cycling stability is poor in carbonate-based electrolytes.
- Ether-based electrolytes improve the cycling stability.
- Specific conductivities of CuS and Cu_2S are determined.

ARTICLE INFO

Article history:
Received 30 July 2013
Received in revised form
27 August 2013
Accepted 29 August 2013
Available online 12 September 2013

Keywords:
Copper sulfide
Displacement reaction
Electrolyte composition
Cycling stability
Lithium batteries

ABSTRACT

Copper sulfides are attractive electrode materials as their reaction with lithium offers high capacity and energy density. However, the reversibility is poor and (nano)structuring is considered necessary to achieve moderate improvements. In contrast, we show in this study that the electrolyte is a major factor that governs the reversibility of the cell reaction. All our experiments were done with commercially available copper sulfides (CuS and Cu_2S) without any special nanostructure. Different electrolyte compositions were tested among $LiPF_6$ in EC/DMC and LiTFSI in DOL/DME. While rapid capacity fading is found in cells containing carbonate-based electrolytes, cells with ether-based electrolytes show a much better electrochemical performance. For a mixture of 1 M LiTFSI in DOL/DME, Cu_2S can be cycled with capacities of around 200 mAh g^{-1} for more than 150 cycles with coulombic efficiencies >98.4%, for example. The improved stability in the ether-based electrolyte further allowed us to study how the discharge and charge voltage change during prolonged cycling. Our study underlines that improvements in the Li/CuS and Li/Cu_2S system are still possible by very simple measures, but further studies on the complex Li–Cu–S phase behavior are necessary to understand the discharging and especially the charging mechanisms.

© 2013 Elsevier B.V. All rights reserved.

1. Introduction

Copper sulfides have been investigated as battery active materials for lithium-ion batteries for several decades. The general characteristics of the cell reactions can be briefly summarized as follows. Reaction of CuS or Cu_2S with lithium to form Cu and Li_2S comes along with an energy release of 961 Wh kg^{-1} or 552 Wh kg^{-1}, respectively. For comparison, commercially applied $Li_{0.5}CoO_2$ theoretically provides 548 Wh kg^{-1}. Besides, copper sulfides are highly conductive which intrinsically should ease the cell reaction compared to many other electrode materials. As the main disadvantage, copper sulfides are known to suffer from poor capacity retention and hence short life time [1,2]. Therefore, they were often considered and used as primary battery materials [3–5]. Several studies were carried out to determine reasons for the poor reversibility [6–8], but precise determination of the reaction mechanisms for the different copper sulfide species has been proven difficult due to the limited cycle life and the existence of several intermediate phases with complex stoichiometries [7,9].

Overall, various factors are thought to be responsible for the poor electrochemical performance of the Li/Cu/S system: (1) loss in structural stability due to volume changes during cycling, (2) decomposition of the electrolyte at the cathode and/or the metallic lithium anode, and (3) loss of active material due to dissolution of sulfide species [4,6–8]. On the other hand, it was reported that the cycling stability of CuS can be improved to some extent by nanostructuring [9–17]. For example, Wang et al. described lately the *in situ* preparation of a nanostructured copper sulfide cathode with an

* Corresponding author. Tel.: +49(0)641 9934501; fax: +49(0)641 9934509.
E-mail address: Philipp.Adelhelm@phys.chemie.uni-giessen.de (P. Adelhelm).

0378-7753/$ – see front matter © 2013 Elsevier B.V. All rights reserved.
http://dx.doi.org/10.1016/j.jpowsour.2013.08.136

excellent stability for more than 100 cycles at different C-rates (up to 2C) with specific capacities between 376 mAh g^{-1} and 447 mAh g^{-1} in a electrolyte composed out of 1 mol L^{-1} $LiClO_4$ and a solvent mixture of DME/DOL (2:1, *v*/*v*) [13]. They concluded that the special nanostructure, which consisted of 3D connected nano-flakes on copper, was the main reason for the improved cycling stability. On the other hand, Han et al. synthesized a CuS material with a hierarchical structure consisting of nano-spheres which only showed a poor cycle life [11]. In an electrolyte composed of 1 M $LiPF_6$ dissolved in EC/DMC (1:1, *v*/*v*), 582 mAh g^{-1} were achieved in the first cycle followed by a rapid decrease of the specific capacity and an overall capacity retention of around 13.8% after the first ten cycles. Débart et al. studied commercial CuS-powders and found nearly the theoretical capacity value during first discharge (1 M $LiPF_6$ in EC/DMC (1:1, *w*/*w*)). However, the capacity rapidly dropped to approx. 50 mAh g^{-1} after five cycles which was related to loss of active mass as a result of Li_2S dissolution in the electrolyte [9]. Altogether it remains unclear whether nanostructuring alone can be linked to an improved cycling stability. And even though also using alternative electrolytes has been suggested in literature as potential method to improve the cycling stability, no correlation could be established either.

In this work, we show that the composition of the electrolyte solution is a major factor that governs the cycle life of copper sulfide in lithium-ion cells, especially when discharged to low potentials. As only commercially available powders are used in our study, we conclude that nanostructuring is probably less important for achieving a stable cycle life. In order to study the reversibility of the cell reaction in more detail, the two copper sulfides CuS and Cu_2S are studied separately. Also the impact of the current collector on the cycling stability is discussed.

2. Experimental

Electrode slurries were made from as received CuS (>99%, *Sigma Aldrich*) or Cu_2S (>99.5%, *Sigma Aldrich*), a conductive carbon (SuperPLi, *TIMCAL Graphite*), polyvinylidene fluoride (PVDF Solef 1310, *Solvay*) and *N*-methyl-2-pyrrolidone (NMP, *Sigma Aldrich*). The content of copper sulfide, conductive carbon and binder was 75 wt%, 15 wt% and 10 wt%, respectively. The electrodes were prepared by doctor blading the slurry onto aluminum foil ($d = 20$ μm). The thicknesses of the electrodes were approximately 200 μm in wet condition and around 40–50 μm in the dried state. Circular electrodes ($d = 1.2$ cm) were punched out and contained between 2 mg and 3 mg of active mass each. The electrodes were further dried at $\vartheta = 80$ °C for 3 h under vacuum to evaporate residual NMP and then transferred to an argon filled glove box (MBraun Labmaster sp) where three-electrode Swagelok type cells were assembled. Metallic lithium foil (*Rockwood Lithium*) was used as counter and reference electrode. Whatman glass microfiber filters (GF/A) were used as separator. As electrolyte three different mixtures of conductive salts and solvents were used. A commercially available 1 M solution of $LiPF_6$ in 1:1 *w*/*w* EC/DMC (LP30, SelectiLyte from *Merck*), a 1 M solution of LiTFSI in 1:1 *w*/*w* DOL/DME (*Sigma Aldrich*) and a 1 M solution of LiTFSI in 1:1 *w*/*w* EC/DMC. Electrochemical measurements were conducted at room temperature using a Maccor (Model 4300) battery cycler. Cells were cycled galvanostatically (constant current, CC) at different C-rates between 0.8 V and 3.0 V. The C-rate was calculated based on the theoretical capacity of CuS ($Q = 560$ mAh g^{-1}) or Cu_2S ($Q = 337$ mAh g^{-1}), i.e. 1C corresponds to a current of $i_{CC} = 560$ mA g^{-1} (CuS) or $i_{CC} = 337$ mA g^{-1} (Cu_2S). Capacities are given in mAh per gram of copper sulfide species (mAh g^{-1} (CuS) or mAh g^{-1} (Cu_2S)). Additionally, cyclic voltammetry was conducted (Biologic VMP3) with a voltage sweep rate of 0.05 mV s^{-1} for 20 cycles. WAXS diffraction patterns were taken with a PANanalytical X'Pert Pro in a 2θ angular range between 20° and 60°.

All samples for conductivity measurement were prepared by pressing the powders into small rods (approx. 3 mm in diameter and 6 mm in length) at 5 kN in a uniaxial press. These rods were used without further treatment. Standard 4-probe measurements were carried out by pressing 4 Pt-wires (0.1 mm) to the pellet within a PTFE sample holder (Fig. 1). The DC conductivities were measured using a Keithley 2420 Sourcemeter. Additional AC measurements were performed with a Novocontrol Alpha-AK/ZG4 system. All experiments were done at room temperature, light exposure was excluded.

3. Results and discussion

3.1. Cell reaction

The basic electrochemical reaction of copper sulfides with lithium is a unique kind of conversion reaction that includes a macroscopic phase separation (a so-called displacement reaction). During discharge, lithium ions diffuse into the copper sulfide lattice leading to the formation of lithium sulfide. At the same time the copper ions diffuse out of the lattice and form macroscopic metallic copper dendrites upon reduction [9]. This behavior is different from the conventional conversion reaction for which a nanocomposite structure is observed that consists of transition metal nanoparticles that are finely dispersed in a Li_aX-matrix ($a = 1,2$ or 3 and X = anions) [1,2]. For the conversion reaction of CuO with lithium one finds Cu nanoparticles dispersed in a Li_2O matrix after discharge, for example. The difference between both mechanisms is illustrated in Fig. 2.

The general discharge profile of the Li/CuS system is characterized by two well defined plateaus and the formation of Li_2S and Cu as the final discharge products. The appearance of a second plateau is indicative for an intermediary phase that has been differently explained literature. Both formation of $Cu_{2-x}S$ phases [3,8,16] and

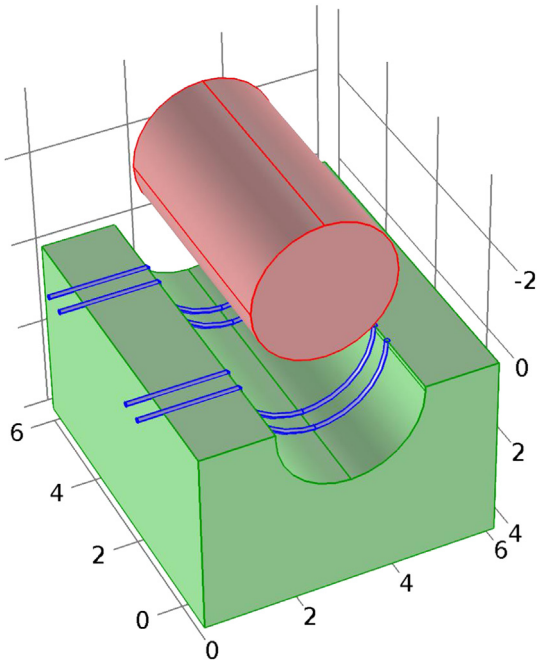

Fig. 1. Sample holder for 4-probe conductivity measurements. Green: PTFE-block; blue: Pt-wires; red: sample rod. All scales in mm. (For interpretation of the references to colour in this figure legend, the reader is referred to the web version of this article.)

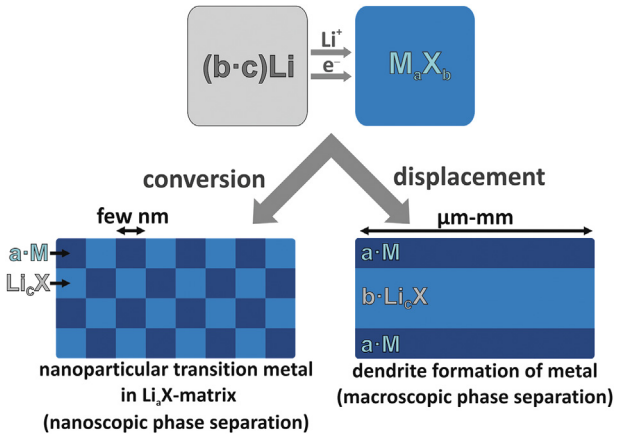

Fig. 2. Schematic drawing of the difference between a conversion [1,2] and a displacement reaction (basic concept based on Ref. [9]). The displacement reaction is typical for copper sulfides. For other species M_aX_b, the conversion reaction involves formation of a nanocomposite structure leading to transition metal nanoparticles dispersed in a Li_cX matrix. $(bc)Li + M_aX_b \leftrightarrow aM + bLi_cX$ with M = transition metal and X = non-metal species.

formation of a $Li_xCu_{1-x}S$ phase as a result of an insertion process [18] have been suggested. Here, it is worth remembering that the oxidation state of Cu in all sulfides is Cu(I) [19,20], so the cell reaction also involves an anion redox chemistry.

Precise analysis of the cell reaction truly is difficult due to the numerous polymorphic structures of $Cu_{2-x}S$ that exist at room temperature [21]. The probably most accurate measurements were provided by the groups of Tarascon [9] and Sohn [16] using a combination of microscopy techniques and *in situ* XRD. Despite some uncertainties, the two plateaus of the discharge reaction can be generalized as follows, with Cu_2S also including stoichiometries $Cu_{2-x}S$:

$$CuS + Li \rightarrow 0.5Cu_2S + 0.5Li_2S \quad (1)$$

$$0.5Cu_2S + Li \rightarrow Cu + 0.5Li_2S \quad (2)$$

Reaction (2) is characterized by the diffusion of lithium ions into a quasi-rigid sulfur sublattice of Cu_2S leading to extrusion of macroscopic copper dendrites, and hence the reaction is labeled as displacement reaction. As a result of this peculiar mechanism, the overpotentials are much smaller compared to what is usually observed for conversion reactions.

Assuming Cu_2S as the only intermediate phase and lithium as anode material, the corresponding theoretical cell potentials and specific capacities can be easily calculated (Table 1). The ideal discharge characteristics would hence exhibit two defined plateaus at 2.14 V and 1.78 V for CuS and only one defined discharge plateau at 1.78 V in case of Cu_2S is used as active material, respectively.

Table 1
Number of transferred electrons, theoretical specific capacities, Gibbs energy and standard electrochemical potential ($T = 298$ K) for different cell reactions of lithium with CuS and Cu_2S. Thermodynamic data was taken from the database of *HSC Chemistry* 7.0.

Reaction step	No. of e^-	Specific capacities /mAh g^{-1}(CuS)	Gibbs energy /kJ mol^{-1}	E°/V
$CuS + Li \rightarrow 1/2Cu_2S + 1/2Li_2S$	1	280.31	−206.85	2.14
$1/2Cu_2S + Li \rightarrow Cu + 1/2Li_2S$	1	280.31 (CuS) [336.78 (Cu_2S)]	−171.97	1.78
Sum: $CuS + 2Li \rightarrow Cu + Li_2S$	2	560.62	−378.82	1.96

These values are in good agreement to what is usually observed in practice. During charging, simply reversing the cell reaction should lead again to two defined plateaus. Experimentally, however, such a two-step behavior is not found and typically several small potential steps followed by one long flat plateau are observed. Even though CuS is found after charging, the cell reaction is not completely reversible and typically around 80% of the discharge capacity is being recovered. The occurrence of several additional steps during charging is not well understood but has been generally related to the formation of a series of copper sulfide intermediate phases [9,16]. Nevertheless, it remains surprising that discharge at defined potentials is followed by a much more complex charging process.

3.2. Reversibility in different electrolytes

A direct comparison between CuS and Cu_2S cathodes cycled in two different electrolyte solutions (LiTFSI/DOL/DME and $LiPF_6$/EC/DMC) is shown in Fig. 3. Two important findings are evident: Firstly, the capacity retention in LiTFSI/DOL/DME (Fig. 3a–c) is much better compared to $LiPF_6$/EC/DMC (Fig. 3d–f). Secondly, while Cu_2S cathodes show stable capacities during prolonged cycling, the capacities of the CuS cathodes decay along with significant shortening of the first plateau at 2.0 V. The disappearance of the first plateau is equatable to a continued cycling mainly between Cu_2S and Cu meaning that the reversible formation of CuS is kinetically less favored. The fact that CuS is electrochemically less active can be well understood when considering boundary conditions necessary for a displacement reaction: (1) Sufficient electronic and ionic conductivity, (2) similar crystal structure and (3) similar molar volumes of the reaction partners. Only the first condition is fulfilled for CuS (Tables 2 and 3), whereas Cu_2S meets all three requirements. This coincidence is quite unique and hence restricted to the reaction of lithium with Cu_2S. For example, replacing lithium by sodium (i.e. considering a Na/Cu_2S cell), leads to a normal conversion reaction as a result of the mismatch between Cu_2S and Na_2S lattice parameters [22]. We note that the Li/Cu_3P system is another example for the important influence of structural similarity on the cycleability of conversion reactions [48].

Even though this explanation seems quite reasonable it still is somewhat surprising as it is known that CuS easily forms from the elements by a chemical solid state reaction even at room temperature. An example is shown in the supporting information where CuS formation from a 1:1 Cu/S mixture within 24 h is evidenced by XRD measurements (Fig. S1). Dispersing sulfur onto copper foil leads to an even more rapid CuS formation (Fig. S2).

The chemical reactivity at room temperature is related to the comparably high mobility of the copper ions in the copper sulfide crystal lattices combined with electronic conductivity. Conductivity values strongly depend on the exact composition and hence the literature data scatters with values for both copper sulfides deviating over three orders of magnitude [23–26]. As a result of this, we decided to separately determine the conductivities of the copper sulfides used in our electrochemical study. Measured in 4-point geometry, both copper sulfides show a linear (i.e. ohmic) current–voltage characteristic in the whole measured current range from ±15 mA to ±100 mA (Fig. S3). This ohmic characteristic was also confirmed by additional AC impedance measurements. For different pellets of the same material we found variations in conductivity values up to a factor of two, mainly dependent on the density of the used pellet. Conductivity values of the samples with the highest density are shown in Table 2 and are in good agreement with 4-probe measurements found in literature [23,24]. For comparison, the electrical and ionic conductivities of the standard cathode materials $LiCoO_2$, $LiMn_2O_4$ and especially $LiFePO_4$ are magnitudes lower [27].

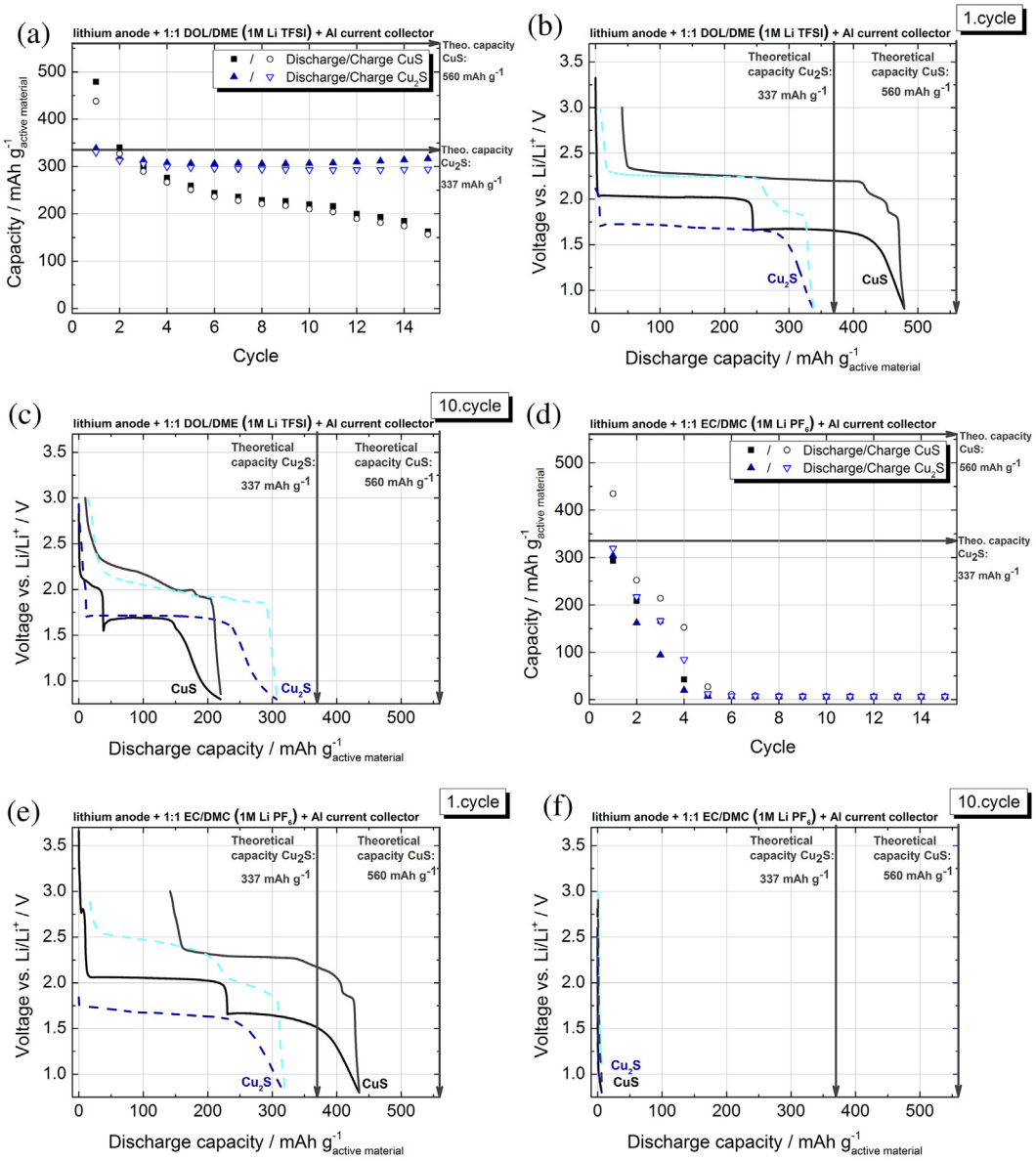

Fig. 3. Comparison of Cu_2S and CuS cathodes cycled in (a)–(c) 1 M LiTFSI/DOL/DME and (d)–(f) 1 M $LiPF_6$/EC/DMC electrolyte during the first 10 cycles.

Evidence for the poor reversibility of CuS can be also seen from XRD measurements, even though it is difficult to analyze the patterns of copper sulfide cathodes after cycling (charged state) due to the low crystallinity of the reaction partners and the combined background noise of carbon additive, binder, current collector and protective foil (a polymer film, used to protect products that are not stable when exposed to air). In Fig. 4 the XRD patterns of the electrodes before (pristine electrodes with CuS and Cu_2S) and after cycling in charged condition are compared for both electrolyte solutions. For the pristine electrodes, the copper sulfides can be well indexed along with the diffraction lines of the carbon additive and the protective foil. The electrodes cycled in $LiPF_6$/EC/DMC show reflexes of the discharge product copper; i.e. the cell reaction is not fully reversible. Also there is hardly any evidence for the charge products. For cathodes cycled in LiTFSI/DOL/DME the result is quite different. For both cathode materials, CuS and Cu_2S, reflexes for Cu_2S as charge product appear, regardless which copper sulfide was used as active material from the start. The results from XRD therefore support the findings from the electrochemical measurements that CuS is poorly reversible compared to Cu_2S.

Table 2
Specific conductivities for CuS and Cu_2S as determined by 4-probe measurements.

Species	Crystallographic density/%	Specific conductivity/S cm^{-1}
CuS	82	870
Cu_2S	84	70

We note that the reversibility of CuS in carbonate-based electrolytes can be improved by reducing the voltage window, i.e. by increasing the lower cut-off voltage to 1.8 V [16]. For our samples, we achieved around 80% of the theoretical capacity for several cycles (Fig. S4). This finding indicates that the poor reversibility of copper sulfides in carbonate-based electrolytes is rooted in irreversible side reactions that predominantly occur during the second discharge step at around 1.78 V.

In order to study whether the conductive salt has any major impact, we screened a number of other different electrolyte

Table 3
Lattice parameters, cell volumes, coordination numbers, space groups, crystal structures and theoretical molar volumes for lithium sulfide, the copper sulfides and copper from the ICSD Database.

Species[ICSD no.]	Lattice parameters/Å	Cell volume/Å^3	No. of formula units per unit cell	Space group	Crystal structure	Molar volume/cm^3 mol^{-1}
Li_2S^{642297}	5.7080	185.97	4	Fm-3m	Anti-fluorite	27.999
Cu_2S^{95398}	5.7620	191.30	4	Fm-3m	Anti-fluorite	28.801
CuS^{628808}	$a = 3.7650$ $c = 16.2900$	199.98	6	P63/mmc	Hexagonal	20.072
Cu^{64699}	3.6150	47.24	4	Fm-3m	Cubic-fcc	7.112

compositions. We found that independent of the type of conductive salt the cycling stability is poor in carbonate-based electrolytes but excellent in DOL/DME based electrolytes (Fig. 5 and Fig. S5). One might also argue that the better reversibility in the ether-based electrolyte is due to its better compatibility with the metallic lithium anode. However, we can safely assume that the anode is not the limiting factor in our experiments, since the same carbonate-based electrolyte works with other active materials such as non-graphitic carbon under identical conditions without any noticeable problems [28–33]. On the other hand, Cu_2O shows a good cycle stability in EC/DMC-based electrolytes [34]. Taking this all together one can conclude that a detrimental side reaction of the carbonate solvent is responsible for the poor capacity retention.

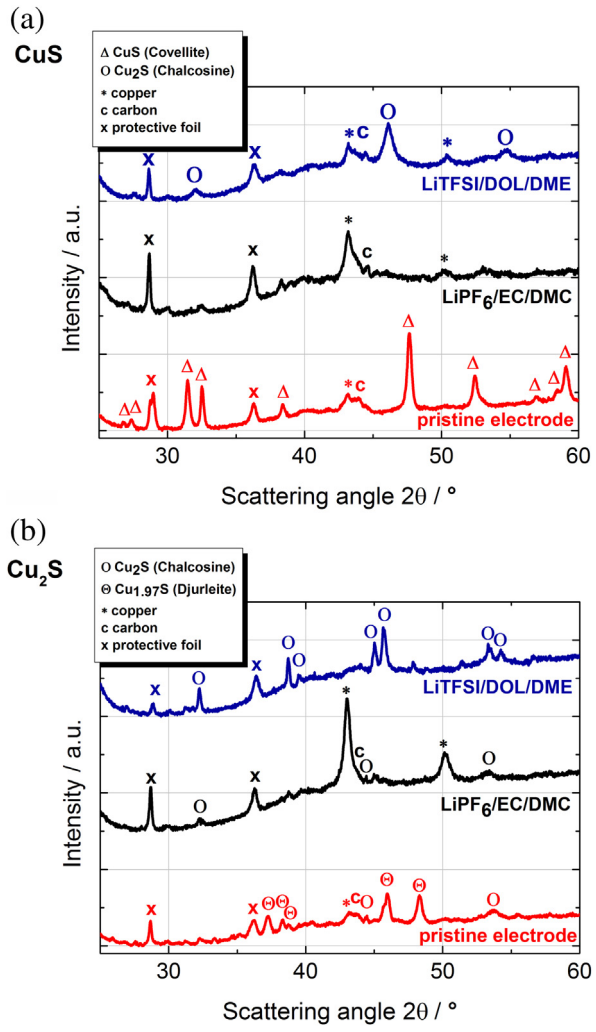

Fig. 4. XRD pattern of (a) CuS and (b) Cu_2S cathodes before and after cycling in different electrolytes at 0.1C rate for 20 cycles (charged state). Due to the low crystallinity only weak diffraction lines are observed.

It has been suggested that the poor reversibility of the CuS system is due to the solubility of the discharge product Li_2S in the electrolyte leading to a rapid loss of active material [9,16,35,36]. Especially polysulfides Li_2S_x that might occur as intermediates during discharge/charge are highly soluble in many solvents and indeed this phenomenon is well-known from the lithium–sulfur cell [37]. Even though we never found evidence for a loss of the active material it is worth considering possible countermeasures (see Section 3.4). In any case, a very recent work on Li/S cells provides direct evidence that polysulfides react with carbonate-based electrolytes via a nucleophilic addition or substitution reaction leading to rapid capacity fading [38]. Hence ether-based electrolytes (DOL/DME) are commonly used in Li/S cells [39,40]. It might well be that the same mechanism is responsible for the poor cycling performance in the Li/Cu/S cells with carbonate-based electrolyte. Besides, one should also bear in mind the well-known instability of EC based electrolytes which undergo electrochemical reduction at low potentials vs. Li/Li^+ and always might lead to stability problems in case of unfavorable SEI formation [41–43].

3.3. Discharge/charge characteristics

Figs. 6 and 7 show data of Fig. 4 that has been replotted for a better discussion of the discharge/charge characteristics. Besides a close look on the first discharge/charge cycle, the improved cycling stability in case of the ether-based electrolyte also allows to study how the voltage profile changes upon prolonged cycling. Complementary cyclic voltammetry measurements were also made (Fig. 8).

3.3.1. CuS – first discharge/charge

During first discharge, the CuS cathodes show a quite similar discharge behavior for both electrolytes with two flat discharge plateaus at around 2.0 V and 1.7 V (Fig. 6a). Both voltage values and the lengths of the plateaus fit well to the two-step discharge mechanism described by Débart et al., where the upper plateau is linked to the formation of polymorphic $Cu_{2-x}S$ and the lower plateau relates to Li_2S formation [9]. Comparing the observed voltage plateaus with the calculated values (Fig. 3), overpotentials in the range of 70 mV are found for the first and second step. The specific capacities are about 480 mAh g^{-1} for the ether-based cells and around 440 mAh g^{-1} for the carbonate-based cells. These values are little lower compared to the theoretical capacity of 560 mAh g^{-1}, indicating that not all CuS was utilized.

During first charging (Fig. 6a) only one extended voltage plateau is observed. This is somewhat unexpected, as also two steps are expected from simply reversing the discharge reaction. Instead, charging starts with a steep increase of the voltage up to around 1.9 V followed by several small steps until reaching a stable

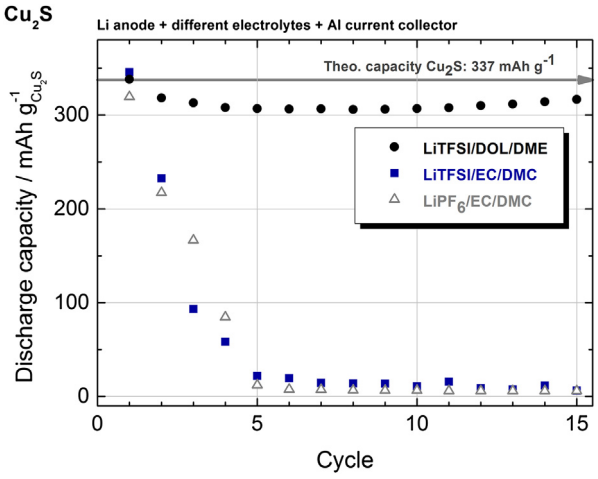

Fig. 5. Specific capacities of Cu_2S cathodes cycled in different electrolytes. The coulombic efficiencies are around >95% for ether-based electrolytes and around >90% for carbonate-based electrolytes.

charging voltage of around 2.25 V. This indicates a different and more complex reaction mechanism for the charge reaction. The finding is well in line with what was earlier observed for the charging process by other groups. A straight forward explanation for the small steps at the beginning of the charge process is the occurrence of several intermediate phases. Nevertheless, these

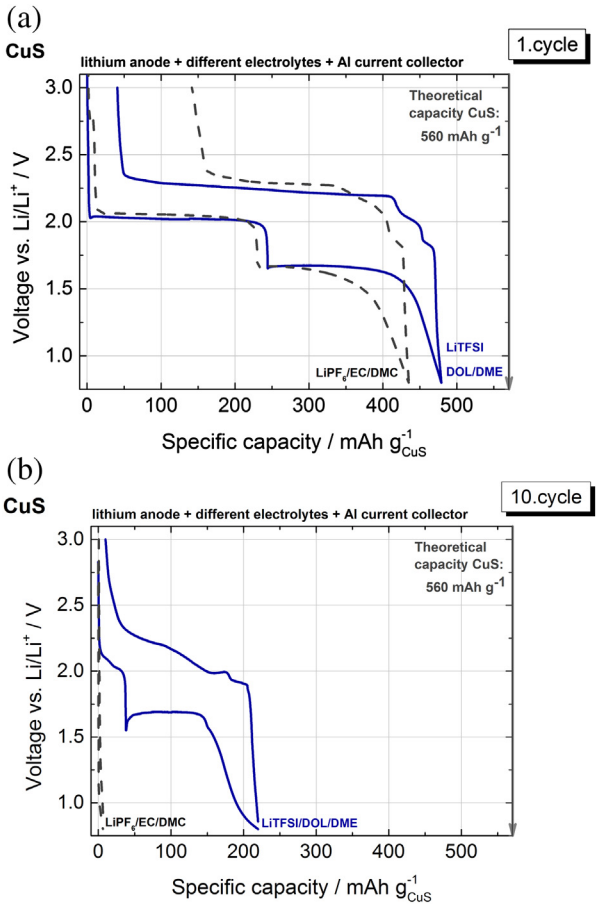

Fig. 6. Discharge and charge characteristic of the (a) first and (b) 10th cycle of CuS cathodes cycled at 0.1C rate in different standard electrolytes in a voltage range of 0.8–3.0 V. The theoretical capacity of CuS is 560 mAh g^{-1}.

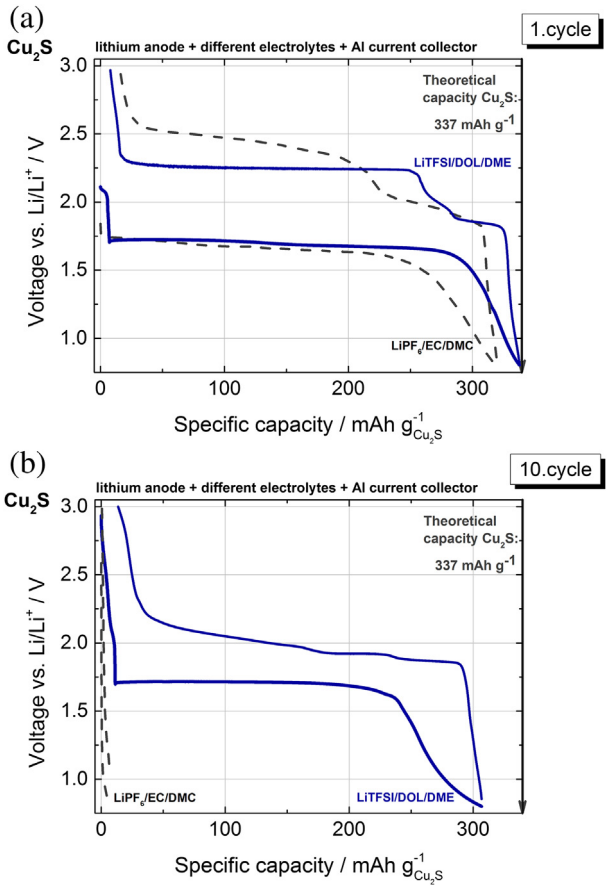

Fig. 7. Discharge and charge characteristic of the (a) first and (b) 10th cycle of Cu_2S cathodes cycled at 0.1C rate in different standard electrolytes in a voltage range of 0.8–3.0 V. The theoretical capacity of Cu_2S is 337 mAh g^{-1}.

steps only contributed to around 10–15% of the total charge capacity, i.e. around 50–60 mAh g^{-1}. To differentiate between the two distinct regions during charging (plateau and steps) the terms “plateau region” and “multi-step region” will be used in the following discussion. To the best of our knowledge, there is no detailed understanding of the underlying mechanisms that occur

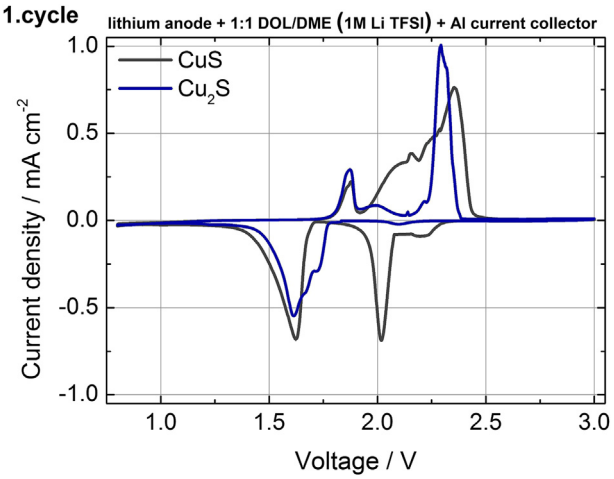

Fig. 8. Cyclic voltammetry with a sweep rate of 0.05 mV s^{-1} and discharge/charge characteristics of Cu_2S and CuS cathodes in a potential range of 0.8–3.0 V in the first cycle. Voltammograms of a CuS and a Cu_2S cathode cycled in LiTFSI/DOL/DME. A CV of a Cu_2S cathode in $LiPF_6$/EC/DMC is shown in the supplementary information Fig. S7.

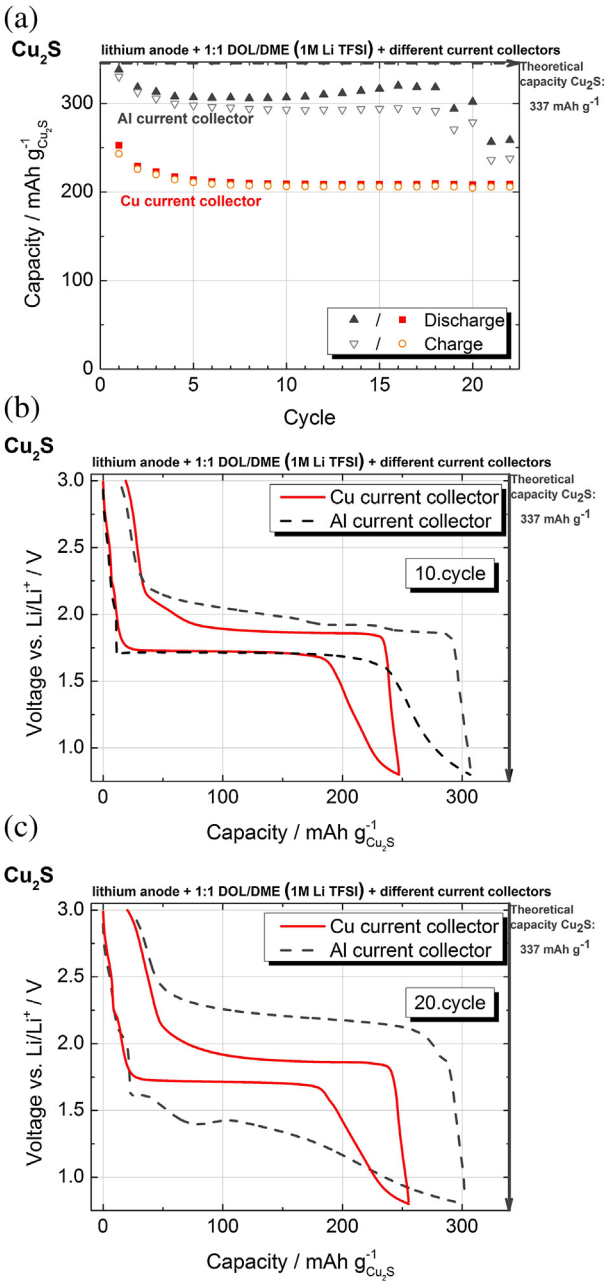

Fig. 9. Cu_2S cathodes galvanostatically cycled on different current collectors. (a) Specific capacities and discharge/charge characteristics in (b) the 10th and (c) the 20th cycle.

during charging and future studies will be necessary to clarify this aspect. For the present study, however, it is enough to note that the mechanisms during beginning of the charging process are similar in both electrolytes. In contrast, the capacity obtained during charging in the plateau region is significantly smaller for the carbonate-based electrolyte, indicating that the poorer reversibility relates to this later reaction mechanism. This is also supported by the higher plateau voltage values in the case of the carbonate-based electrolyte (2.45 V vs. 2.25 V). The difference of 200 mV indicates a higher internal resistance eventually caused by a passivating interface.

3.3.2. CuS – subsequent cycling

The discharge and charge curves of the 10th cycle are shown in Fig. 6b. Compared to the first discharge, the capacity in the carbonate-based electrolyte is negligible, so these results will be not further discussed. For the ether-based electrolyte, the first plateau significantly shortened and is shifted toward higher potentials. Almost all capacity is obtained in the second plateau region down to the cut-off potential. The second plateau is initiated by a sharp minimum indicative for a nucleation process. Even more different is the slope of the charging curve: The charging plateau region at around 2.25 V nearly vanished and nearly all capacity is obtained in the multi-step region (Fig. 6b). Remembering that this region only contributed around 50–60 mAh g^{-1} to the total capacity during first charge it is surprising that this region now contributes around 200 mAh g^{-1}. Obviously, the cell reaction proceeds more and more over intermediate phases as cycling numbers increase. However, the enduring occurrence of a discharge plateau at around 1.7 V also indicates defined chemical potentials during larger parts of the discharge process.

3.3.3. Cu_2S

Fig. 7 shows the analog graphs for Cu_2S cycled in the same potential window. As expected, the first plateau is missing during first discharge and all capacity is obtained at a constant voltage plateau close to the value when starting off with CuS (Fig. 7a). Charging proceeds very similar to what was found for the CuS electrodes, i.e. a multi-step region is followed by a plateau region of constant potential. For the ether-based electrolyte, the charging potential is identical irrespective of the type of copper sulfide used from the start (see Fig. S6 for comparison). After ten cycles, again the plateau region has vanished and most of the capacity is obtained in the multi-step region (Fig. 7b). Even though the charging mechanisms

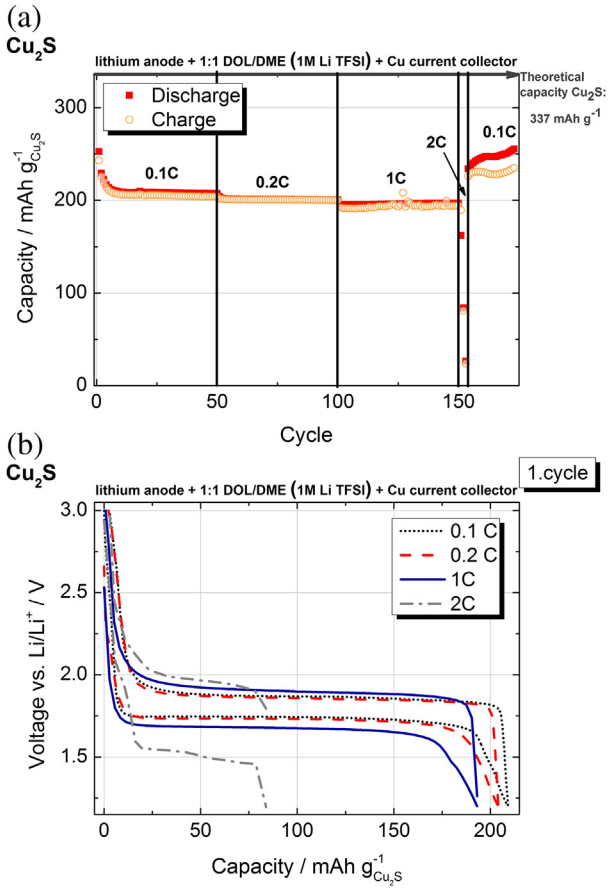

Fig. 10. Specific capacities of a Cu_2S cathode measured at different C-rates in a potential range of 0.8–3.0 V.

seem identical for both electrodes, the Cu_2S electrode exhibits a superior cycling stability. Again, the cycling stability of Cu_2S in the carbonate-based electrolyte is poorer compared to the ether-based electrolyte.

The differences between discharge and charge mechanisms can be also seen from cyclic voltammetry. The CVs obtained for the CuS and Cu_2S cathodes cycled in LiTFSI/DOL/DME are shown in Fig. 8. The discharge process for both electrodes is characterized by one (Cu_2S) respectively two (CuS) defined potentials. The charging proceeds in both cases over several smaller peaks (multi-step region) followed by a defined large peak (plateau region). The characteristics of the voltammograms match well to the results obtained for the galvanostatic cycling mode.

In conclusion, the most relevant finding is that using an ether-based electrolyte significantly improves the cycling stability of copper sulfides and no nanostructuring seems necessary to obtain a good reversibility. The improved cycling stability allows studying changes in reaction mechanisms during subsequent cycling, however we obtained puzzling results that underline the complexity of the cell reaction between lithium and copper sulfides. The findings from our electrochemical studies can be summarized as follows:

(1) The first discharge of a CuS electrode proceeds over the expected two-step discharge mechanism with an upper and a lower plateau that are close to what is expected from thermodynamics assuming formation of a Cu_2S species as intermediate and Cu and Li_2S as final discharge products. Accordingly, only one voltage plateau is observed when starting from Cu_2S.
(2) Upon subsequent cycling of CuS electrodes, the upper plateau diminishes while *the lower plateau maintains constant* at the same voltage values in a large capacity range. This indicates that the reduction of CuS to $Cu_{2-x}S$ is kinetically not favored, which can be understood from the differences in the crystallographic nature of both compounds (see discussion above).
(3) Charging proceeds very different from discharging and it is very similar for CuS and Cu_2S electrodes. For both electrodes, charging starts with a multi-step region starting from around 1.6 V that is followed by only one plateau region with a defined potential at around 2.25 V. Initially, the multi-step region contributes only little to the total reversibly capacity (several tens of mAh g^{-1}) but after a few cycles almost all charging capacity (few hundred mAh g^{-1}) is obtained in this region.
(4) Three aspects are surprising: Firstly, even though the charging voltage plateau is replaced by a multi-step region, the discharge plateau remains unaffected. Secondly, the voltage range of the multi-step region lies below the voltage plateau, i.e. the charging voltage decreases by time. Thirdly, as the charging potential is the same for CuS and Cu_2S electrodes, one would assume the same charging product. However, CuS electrodes cycle less well compared to Cu_2S electrodes. Clearly, explaining these findings necessitates a much more detailed analysis in the future.

3.4. Copper current collector

As already discussed before, the poor reversibility of the CuS system has been related to the solubility of sulfide species in the electrolyte solution that causes a continuous and rapid loss of active material during cell cycling. Even though we did not find direct evidence for this in our experiments it is worth considering this possible degradation mechanism. The question therefore is how eventual dissolution of sulfide species into the electrolyte can be effectively prevented. A simple solution to this could be to replace the commonly used aluminum cathode current collector by copper. It is well-known that CuS can be prepared by simply immersing metallic copper into organic solutions containing polysulfides [7]. Using copper as cathode current collector in a Li/CuS cell will hence provide a dual function: (1) electron conduction and (2) trapping of dissolved sulfide species to reform copper sulfide. The latter effect can be effectively demonstrated in lithium/sulfur cells for which dissolution of polysulfides is a well-known phenomenon. If aluminum is used as current collector, parts of the dissolved polysulfides deposit on the cell separator which can be easily seen after re-opening a cycled cell. No such deposits are found in case copper is used as current collector evidencing its polysulfide captivating nature (Fig. S8). Replacement of Al by Cu as current collector is possible because Cu is electrochemically stable within the applied voltage window. In Li-ion conducting electrolytes, Cu is stable up to around 3.6 V vs. Li/Li^+ [44].

The influence of the current collector on the cycling performance is shown in Fig. 9. Higher capacities were obtained when using Al as current collector with values around 300 mAh g^{-1} during the first cycles compared to around 220 mAh g^{-1} for Cu. On the other hand, the cycling stability was better when using Cu as current collector. More importantly, the type of current collector has a major influence on the overpotentials during charge and discharge. For aluminum, a continuous increase is observed and the combined overpotentials amount to around 1 V after 20 cycles. For copper, the combined overpotentials are constantly in the range of only 200 mV. As copper and aluminum current collectors do not show the same surface and morphology (Al current collectors need to be etched prior coating and Cu current collectors exhibit a rough surface structure for improved adhesion, Fig. S9) a direct link on the impact on the capacity values is difficult. Nonetheless the high coulombic efficiency for the Cu current collector indicates that indeed no active material is lost due to dissolution into the electrolyte solution. But also the excess of copper that is introduced might benefit the overall reversibility of the cell reaction. The increase in cell polarization observed for the cell with Al current collector can be most certainly related to the known corrosion of Al in LiTFSI containing electrolytes that results in surface passivation and hence and increased resistance [44–47]. Overall, we found that using Cu as current collector is beneficial to the cell performance. We note that CuS electrodes can be also directly prepared by casting a conventional slurry containing sulfur, carbon and binder onto a copper current collector. CuS formation occurs immediately and the resulting composite electrode shows the exact same characteristics during cycling as compared to when a CuS/carbon/binder slurry is used.

3.5. Rate capability and prolonged cycling

Rate capability and long term cycling stability were tested for the cell assembly that showed the best overall performance, *i.e.* Cu_2S electrodes were cycled using copper as current collector and LiTFSI in DOL/DME as electrolyte. Cells were cycled at C-rates of 0.1C, 0.2C, 1C and 2C (Fig. 10). Excellent capacity retention for at least 150 cycles and coulombic efficiencies exceeding 98.4% were obtained when cycling the cells at 1C or below. The obtained capacities correspond to about 60% of the theoretical value; even at a 1C rate. Raising the current to 2C leads to a rapid and continuous capacity loss. Further, the cathode becomes irreversible damaged.

4. Conclusion

The cycling stability of commercially available copper sulfides against lithium was investigated in different electrolytes. A very poor cycling stability is found for carbonate-based electrolytes

which is in line with earlier reports on this cell system that date back to the 1970s. However, a much improved cycling stability can be obtained when using an ether-based solvent (1 M LiTFSI in DOL/DME). Cu_2S could be cycled for more than 150 times with coulombic efficiencies exceeding 98% and combined overvoltages of only around 200 mV at different C-rate up to 1C, for example. From this it follows that not the nanostructure/morphology is the key factor governing the cycling stability of copper sulfides as secondary battery material, but instead the choice of an appropriate electrolyte. Even though many reports on the influence of electrolyte compositions on the cycling performance of electrode materials exist, it is surprising that, to the best of our knowledge, such a link was not reported for copper sulfides yet. The improved cycling stability also permits to have a closer look on how the voltage profiles and active species change with time. Starting from CuS, the initially two-step discharge mechanism over a Cu_2S intermediate is replaced by a one-step mechanism (Cu_2S only) after a few cycles. This effect is very pronounced and leads to a disappearance of all existing CuS in the assayed electrode. Charging is found to be very complex. During the first cycles, charging of both CuS and Cu_2S electrodes mostly occurs at a defined voltage plateau. Surprisingly, this plateau is completely replaced by a multi-step region at lower voltages upon subsequent cycling. The underlying mechanisms remain unclear but they are likely related to the known complexity of the Cu–S phase diagram which is further complicated by interaction with lithium.

In summary it can be concluded that the electrochemical performance of the copper sulfides is directly linked to the composition of the chosen electrolyte. Despite the comparably low average cell voltages obtainable, CuS and Cu_2S remain interesting electrode materials due to their high capacity, high intrinsic conductivity and the unique displacement mechanism with lithium that proceeds at overpotentials much smaller compared to other conversion reactions.

Acknowledgments

We thank Dr. Amrtha Bhide and M. Pavlis for experimental support and Prof. Janek for scientific discussion. Financial support is gratefully acknowledged from the state of Hessen (Landes-Offensive zur Entwicklung Wissenschaftlich-ökonomischer Exzellenz (LOEWE)) within the project Store-E (Stoffspeicherung in Grenzflächen).

Appendix A. Supplementary data

Supplementary data related to this article can be found at http://dx.doi.org/10.1016/j.jpowsour.2013.08.136.

References

[1] R. Malini, U. Uma, T. Sheela, M. Ganesan, N.G. Renganathan, Ionics 15 (2009) 301.
[2] J. Cabana, L. Monconduit, D. Larcher, M.R. Palacin, Adv. Mater. 22 (2010) E170.
[3] J.P. Gabano, V. Déchenaux, G. Gerbier, J. Jammet, J. Electrochem. Soc. 119 (1972) 459.
[4] G. Eichinger, H.P. Fritz, Electroanal. Chem. Interfac. Electrochem. 58 (1975) 357.
[5] A. Etienne, J. Electrochem. Soc. 117 (1970) 870.
[6] F.W. Dampier, J. Electrochem. Soc. 128 (1981) 2501.
[7] G. Eichinger, H.P. Fritz, Electrochim. Acta 20 (1974) 753.
[8] F. Bonino, M. Lazzari, B. Rivolta, B. Scrosati, J. Electrochem. Soc. 131 (1984) 1498.
[9] A. Débart, L. Dupont, R. Patrice, J.-M. Tarascon, Solid State Sci. 8 (2006) 640.
[10] H. Mazor, D. Golodnitsky, L. Burstein, E. Peled, Electrochem. Solid State Lett. 12 (2009) A232.
[11] Y. Han, Y. Wang, W. Gao, Y. Wang, L. Jiao, H. Yuan, S. Liu, Powder Technol. 212 (2011) 64.
[12] Y.H. Chen, C. Davoisne, J.M. Tarascon, C. Guery, J. Mater. Chem. 22 (2012) 5295.
[13] Y. Wang, X. Zhang, P. Chen, H. Liao, S. Cheng, Electrochim. Acta 80 (2012) 264.
[14] L. Zhao, F.Q. Tao, Z. Quan, X.L. Zhou, Y.H. Yuan, J.C. Hu, Mater. Lett. 68 (2012) 28.
[15] R. Cai, J. Chen, J. Zhu, C. Xu, W. Zhang, C. Zhang, W. Shi, H. Tan, D. Yang, H.H. Hng, T.M. Lim, Q. Yan, J. Phys. Chem. C 116 (2012) 12468–12474.
[16] J.S. Chung, H.J. Sohn, J. Power Sourc. 108 (2002) 226.
[17] A. Hayashi, R. Ohtsubo, T. Ohtomo, F. Mizuno, M. Tatsumisago, J. Power Sourc. 183 (2008) 422.
[18] R. Fournie, R. Messina, J. Perichon, J. Appl. Electrochem. 9 (1979) 329.
[19] S.W. Goh, A.N. Buckley, R.N. Lamb, R.A. Rosenberg, D. Moran, Geochim. Cosmochim. Acta 70 (2006) 2210.
[20] S.W. Goh, A.N. Buckley, R.N. Lamb, Miner. Eng. 19 (2006) 204.
[21] D.J. Chakrabati, D.E. Laughlin, Bull. of Alloy Phase Diagrams 4 (1983) 254.
[22] F. Klein, B. Jache, A. Bhide, P. Adelhelm, Phys. Chem. Chem. Phys. 15 (2013) 15876–15887.
[23] H. Fjellvåg, F. Grønvold, S. Stølen, A.F. Andresen, A. Müller-Käfer, Reinhold Simon, Z. Kristallogr. – Crystal. Mater. 184 (1988) 111.
[24] K. Okamoto, S. Kawai, Jpn. J. Appl. Phys. 12 (1973) 1130.
[25] H. Grijalva, O.M. Inoue, S. Boggavarapub, P. Calved, J. Mater. Chem. 6 (1996) 1157.
[26] J.B. Wagner, C. Wagner, J. Chem. Phys. 26 (1957) 1597.
[27] M. Park, X. Zhang, M. Chung, G.B. Less, A.M. Sastry, J. Power Sourc. 195 (2010) 7904.
[28] B. Jache, C. Neumann, J. Becker, B.M. Smarsly, P. Adelhelm, J. Mater. Chem. 22 (2012) 10787.
[29] H. Buqa, D. Goers, M. Holzapfel, M.E. Spahr, P. Novak, J. Electrochem. Soc. 152 (2005) A474.
[30] J.R. Dahn, T. Zheng, Y.H. Liu, J.S. Xue, Science 270 (1995) 590.
[31] W. Markle, N. Tran, D. Goers, M.E. Spahr, P. Novak, Carbon 47 (2009) 2727.
[32] M. Winter, J.O. Besenhard, M.E. Spahr, P. Novak, Adv. Mater. 10 (1998) 725.
[33] Y.S. Hu, P. Adelhelm, B.M. Smarsly, S. Hore, M. Antonietti, J. Maier, Adv. Funct. Mater. 17 (2007) 1873.
[34] S. Grugeon, S. Laruelle, R. Herrera-Urbina, L. Dupont, P. Poizot, J.-M. Tarascon, J. Electrochem. Soc. 148 (2001) A285.
[35] A. Eichhöfer, H. Sommer, V. Andrushko, S. Indris, S. Malik, Eur. J. Inorg. Chem. 2013 (2013) 1531.
[36] S. Indris, J. Cabana, O.J. Rutt, S.J. Clarke, C.P. Grey, JACS Commun. 128 (2006) 13354.
[37] K. Abraham, J. Power Sourc. 7 (1982) 1.
[38] T. Yim, M.-S. Park, J.-S. Yu, K.J. Kim, K.Y. Im, J.-H. Kim, G. Jeong, Y.-N. Jo, S.-G. Woo, K.S. Kang, I. Lee, Y.-J. Kim, Electrochim. Acta (2013), http://dx.doi.org/10.1016/j.electacta.2013.06.039.
[39] Y.V. Mikhaylik, I. Kovalev, R. Schock, K. Kumaresan, J. Xu, J. Affinito, ECS Trans. 25 (2010) 23.
[40] E. Peled, Y. Sternberg, A. Gorenshtein, Y. Lavi, J. Electrochem. Soc. 136 (1989) 1621.
[41] D. Aurbach, M. Moshkovich, Y. Cohen, A. Schechter, Langmuir 15 (1999) 2947.
[42] X. Zhang, R. Kostecki, T.J. Richardson, J.K. Pugh, P.N. Ross, J. Electrochem. Soc. 148 (2001) A1341.
[43] S. Mori, H. Asahina, H. Suzuki, A. Yonei, K. Yokoto, J. Power Sourc. 68 (1997) 59.
[44] S.-T. Myung, Y. Hitoshi, Y.-K. Sun, J. Mater. Chem. 21 (2011) 9891.
[45] V. Aravindan, J. Gnanaraj, S. Madhavi, H.K. Liu, Chemistry 17 (2011) 14326.
[46] K. Xu, Chem. Rev. 104 (2004) 4303.
[47] K. Naoi, J. Electrochem. Soc. 146 (1999) 462.
[48] M.P. Bichat, T. Politova, J.L. Pascal, F. Favier, L. Monconduit, J. Electrochem. Soc. 151 (2004) A2074–A2081.